

1 **Risks in signal processing pipelines influencing the estimation of phase**
2 **dependency for EEG-TMS**

3

4 Robert Guggenberger*, Maximilian Scherer, Alireza Gharabaghi*

5 Division of Functional and Restorative Neurosurgery, and Tuebingen Neuro Campus,
6 Eberhard Karls University Tuebingen, Tuebingen, Germany

7 *To whom correspondence should be addressed

8 Dr. Robert Guggenberger and Professor Alireza Gharabaghi, Division of Functional
9 and Restorative Neurosurgery, Eberhard Karls University Tuebingen, Otfried-Mueller-
10 Str.45, 72076 Tuebingen, Germany. Email addresses: robert.guggenberger@uni-
11 tuebingen.de and alireza.gharabaghi@uni-tuebingen.de

12

13 **Acknowledgments**

14 M.S. was supported by the Graduate Training Centre of Neuroscience &
15 International Max Planck Research School, Graduate School of Neural Information
16 Processing, Tuebingen, Germany. A.G. was supported by grants from the German
17 Federal Ministry of Education and Research [BMBF 13GW0119B, IMONAS;
18 13GW0214B, INSPIRATION; 13GW0270B, INAUDITAS] and the Baden-
19 Wuerttemberg Foundation [NEU005, NemoPlast]. The authors declare no competing
20 financial interests.

21

22 **Abstract**

23 Phase-dependency of cortico-spinal excitability can be researched using TMS-EEG.
24 Due to the large artifact, non-causal filters can smear the TMS artifact and distort the
25 phase. However, causal filters can become biased by too high filter orders or uneven
26 pass-bands. We explored the influence of different signal processing pipelines on the
27 estimation of the optimal phase. This exploration involved performing two simulation
28 studies. In the first, we simulated two different phase-dependencies (uni- versus
29 bimodal) and sought to recover them with two distinct approaches that have previously
30 been described. In the second, we specifically explored how filter parameters (e.g.,
31 order, pass-band) biased the phase estimation. On the basis of these findings, we
32 propose using up-to-date toolboxes, re-running scripts after software updates and
33 performing simulation studies in parallel to safeguard the analysis pipeline of empirical
34 studies.

35 **Keywords:** phase dependency, transcranial magnetic stimulation, motor-evoked
36 potential, digital signal processing, brain-state-dependent stimulation

37 Introduction

38 The excitability of neuronal populations depends on their current state (Izhikevich,
39 2007). The use of non-invasive measurements to monitor the current state of neuronal
40 populations is an important step towards implementing brain-state-dependent
41 transcranial stimulation for research and therapy. This is feasible with power-based
42 approaches. For example, desynchronization of sensorimotor power, as picked up by
43 electroencephalography (EEG), increases cortico-spinal excitability (CSE), as
44 measured by the motor-evoked potential (MEP) in response to transcranial magnetic
45 stimulation (TMS; Takahashi et al., 2018; Takemi et al., 2013; Kraus et al., 2016,
46 2018). Similarly, transcranial alternating current stimulation (tACS), which is assumed
47 to synchronize neuronal populations (Zaehle et al., 2010), is able to increase CSE.
48 Such knowledge has already been used to implement interventions for clinical
49 application (Gharabaghi et al., 2014).

50 Most TMS devices that apply short-lasting single pulses can be triggered with very
51 short latencies. Such high temporal precision makes it possible to probe the state-
52 dependency of CSE not only with respect to the rather slow-changing measure of
53 oscillatory power but also with regard to the relatively fast-changing phase of an
54 oscillation. Research has suggested that the use of TMS at different phases of
55 sinusoidal signals applied via transcranial alternating current stimulation (tACS)
56 discloses such phase-dependency of CSE (Raco et al., 2016; Guerra et al., 2016;
57 Nakazono et al., 2016; Fehér et al., 2017; Schilberg et al., 2018).

58 The step from exogenous entrainment of oscillations via tACS to reading the current
59 endogenous phase of an oscillation from EEG or EMG recordings entails several
60 challenges. Unlike a tACS signal, the signal-to-noise ratio of non-invasive
61 electrophysiological recordings is low. The amplitude and phase of oscillations are
62 non-stationary and might be sinusoidal only in approximation (Cole and Voytek, 2017).
63 In an attempt to address this non-stationarity, the construction of dedicated hardware
64 might become necessary for fast processing. However, despite using dedicated
65 hardware, and even if performed only when the oscillation amplitudes are high, real-
66 time estimation of an oscillations phase might have a standard deviation of about 50°
67 (Zrenner et al., 2017).

68 Post-hoc analysis of TMS, applied initially at random and subsequently probed for
69 possible phase-dependencies, therefore remains an important method of research
70 (van Elswijk et al., 2010; Keil et al., 2013; Khademi et al., 2018). Nonetheless, this
71 approach still requires the stringent design of a signal processing pipeline with a
72 special focus on the filter design. For example, non-causal filters may smear the TMS
73 artifact and distort the phase of an oscillation prior to the TMS pulse. Furthermore,
74 when transferred to real-time applications, only causal filters are feasible. In this study,
75 we show how methodological differences in the design of causal filters affect the
76 estimation of the phase dependency. This is not simply a methodological question.
77 For example, with regard to the phase-dependency in the oscillatory beta-band, it is
78 unclear as to whether there is only one maximum of CSE, found in the rising phase of
79 an oscillation (Khademi et al., 2018; van Elswijk et al., 2010), or whether there are two
80 maxima of CSE, i.e., at the peak and trough of an oscillation (Keil et al., 2013). Using
81 simulated data, we show how two different approaches of phase estimation can result
82 in such conflicting findings, even when based on identical data. Subsequently, we
83 explore the general influence of the filter order and bandwidth on recovering the phase

84 of maximal CSE. Finally, we discuss policies for minimizing risks in the design and
85 implementation of signal processing pipelines for estimation of phase dependency.

86 **Material and Method**

87 All simulations were performed and visualized with Anaconda Python 3.6.5 on Linux
88 Mint 18.2, employing SciPy 1.1.0, NumPy 1.14.3, Seaborn 0.8.1 and Matplotlib 2.2.2.
89 The script to create simulated dependencies is available online (<https://osf.io/mgu4h/>).

90 **Simulation 1**

91 We simulated data with two dependencies between oscillatory phase and MEP
92 amplitude. One was bimodal, i.e., with two maxima of MEP at peak and trough of the
93 oscillation. The other was unimodal, i.e., with only a single maximum at the rising flank.
94 Both dependencies were sampled, filtered and processed in accordance with the
95 methods reported previously (Keil et al., 2013; van Elswijk et al., 2010).

96 *Data model*

97 In the dependency models, data was simulated as a 18 Hz cosine signal, and
98 subsequent analyses were performed in accordance with two previous reports. The
99 first approach involved estimating the phase in analogy to Keil and colleagues (Keil et
100 al., 2013) on the basis of a Hilbert transformation. We simulated the data with a 2 kHz
101 sampling rate and duration of ± 1.5 s, and included three cycles, terminating 5 ms
102 before the TMS pulse. The second approach entailed estimating the phase in analogy
103 to Elswijk and colleagues (van Elswijk et al., 2010) on the basis of a discrete Fourier
104 transformation. We simulated the data with a 10 kHz sampling rate and duration of \pm
105 1.1 s, and included two cycles prior to the TMS pulse.

106 *MEP dependency*

107 We simulated two different dependencies between the oscillatory phase and MEP
108 amplitude: maximum MEP amplitude (i) with a unimodal pattern, i.e., at the *rising*
109 phase of 18 Hz oscillations, (ii) with a bimodal pattern, i.e., at the peak and trough of
110 18 Hz oscillations. We simulated a log-linear relationship with base 50 to account for
111 the log-normal distribution of MEPs. The two dependency models are presented in
112 figure 1A.

113 *Filter Order*

114 Simulated data epochs were bandpass filtered forward in time with a Butterworth filter
115 with orders from 0 to 8, and for two different frequency bands depending on the
116 approach, i.e., 10-400 Hz (van Elswijk et al., 2010) or 17-19 Hz (Keil et al., 2013).

117 *Assessment*

118 We visualized the simulation results as polar-linear and linear-linear scatter plots
119 between oscillatory phase and MEP amplitude. To achieve a well-resolved and
120 uniform sampling across the unit circle, the relationship for each integer phase was
121 sampled from 0° to 360° . For the simulation, we added a small white noise term (with
122 0.05 standard deviation) to prevent points from overlaying and to reduce any possible
123 bias due to numerical errors.

124 **Simulation 2**

125 We simulated data as above, but with one dependency mode only, i.e., peak of CSE
126 would be at the rising flank of an oscillation at 18 Hz. Signals were simulated with a
127 sampling rate of 1000 Hz, for the duration of ± 1.5 s around the TMS for filtering, and
128 included three cycles for subsequent phase estimation. The signal was simulated
129 without noise.

130 *Data processing*

131 We filtered the data by exploring the influence of four parameters, i.e., *estimation*
132 *method*, *filter order*, *filter bandwidth*, and *filter center*. The phase was estimated using
133 either Hilbert or Fourier transformation as described above. Additionally, we
134 systematically increased filter order up to an order of 8, and decreased the filter
135 bandwidth. This was achieved in two ways, with the bandwidth (i) centered on the
136 frequency of interest, and (ii) unevenly anchored.

137 *Assessment*

138 We visualized the simulation results as heat maps, showing the phase which was
139 estimated to exhibit a maximal MEP after filtering.

140 **Results**

141 **Simulation study 1**

142 Our first simulation contrasted a narrow-band centered filter of high order followed by
143 Hilbert transformation (approach 1) with a broad-band unevenly anchored filter of
144 lower order followed by Fourier transformation (approach 2). It suggested that the
145 second approach achieves better recovery of the original dependency. The first
146 approach was unable to recover a unimodal phase-dependency of MEP amplitudes,
147 while the second was able to discern between uni- and bimodal phase dependencies
148 (see figure 1 B/C). Only when the order of the narrow-band filter was decreased did
149 this approach recover a unimodal phase dependency (see figure 1 D) and distinguish
150 it from a bimodal phase dependency (see figure 1 E).

151 **Simulation study 2**

152 This simulation explored how the estimation of the optimal phase in the case of
153 unimodal dependency was affected by various parameters of the signal processing
154 pipeline. It highlighted that the phase, whether estimated with Hilbert (see figure 2 A/C)
155 or Fourier transformation (see figure 2 B/D), appears to exhibit similar profiles. The
156 main issue comes with higher filter orders by starting to distort the signal; a
157 phenomenon which appears to start earlier for more narrow bands. At the same time,
158 running a causal filter with an uneven bandwidth can bias the optimal phase estimate
159 significantly (see figure 2 C/D).

160 **Discussion**

161 We conducted two simulation studies to explore how differences in signal processing
162 affect the estimation of phase-dependency. The first of these studies applied two
163 approaches based on earlier research (Keil et al., 2013; van Elswijk et al., 2010). The
164 second explored the influence of processing on the phase estimation. The goal was to

165 investigate how differences of data processing can explain supposedly contradictory
166 findings in earlier literature, and explore the related pitfalls.

167 *Methodological considerations*

168 One key result of our simulation studies was that a low filter order is required to
169 recover uni- and bimodal phase-dependency patterns. If filter orders are too high, the
170 signal becomes distorted, which in turn leads to an artifactual bimodal dependency
171 (see figure 1 D/E). Given a sufficiently low order, both broad-band Fourier and narrow-
172 band Hilbert transformation were able to recover the original phase-dependent
173 relationship. The apparently bimodal dependency introduced by filtering is mainly
174 artifactual, given that too high filter orders can corrupt the phase spectrum of a signal
175 (Oppenheim et al., 2014).

176 At the same time, applying causal filters with uneven pass-bands induces phase-
177 shifts. An evenly centered passband should therefore be considered as a step towards
178 minimizing phase distortion, should a specific frequency be of interest.

179 More generally, if Hilbert transformation is used for phase-estimation, this can clash
180 with the goal of estimating the phase for a narrow frequency band of interest. In such
181 cases, phase estimation using Fourier transformation after broad-band low-order
182 filtering might constitute a more suitable approach.

183 It should also be noted that using a temporal lag in relationship to the MEP necessarily
184 introduces a phase-shift (see figure 1 D/E). For example, 5 ms at a frequency of 18 Hz
185 correspond to $\sim 32^\circ$. Correcting for this can be challenging. If the frequency is
186 determined a priori, correcting the bias may be a good alternative. However, if more
187 non-stationarity is required, unsupervised phase prediction, e.g., the use of an
188 adaptive autoregressive model (Zrenner et al., 2017) might also be considered as a
189 feasible option.

190 *Toolbox selection*

191 Implementations of the same processing pipeline in different environments, e.g., by
192 using different toolboxes or programming languages, can influence the results
193 (Widmann et al., 2015). Notably, recent versions of a commonly used data analysis
194 software (Fieldtrip, Oostenveld et al., 2011) support an automatic filter instability
195 correction and interrupt the computation (e.g., “*fail with an exception*”), if the filter
196 order is too high. This behavior was introduced in early 2013 (according to git log-grep
197 “instability”, commit #914d6ab, <https://github.com/fieldtrip/fieldtrip/>); analyses
198 performed prior to this software update might therefore not have experienced any error
199 warning if the applied filter orders were too high.

200 *Conclusions*

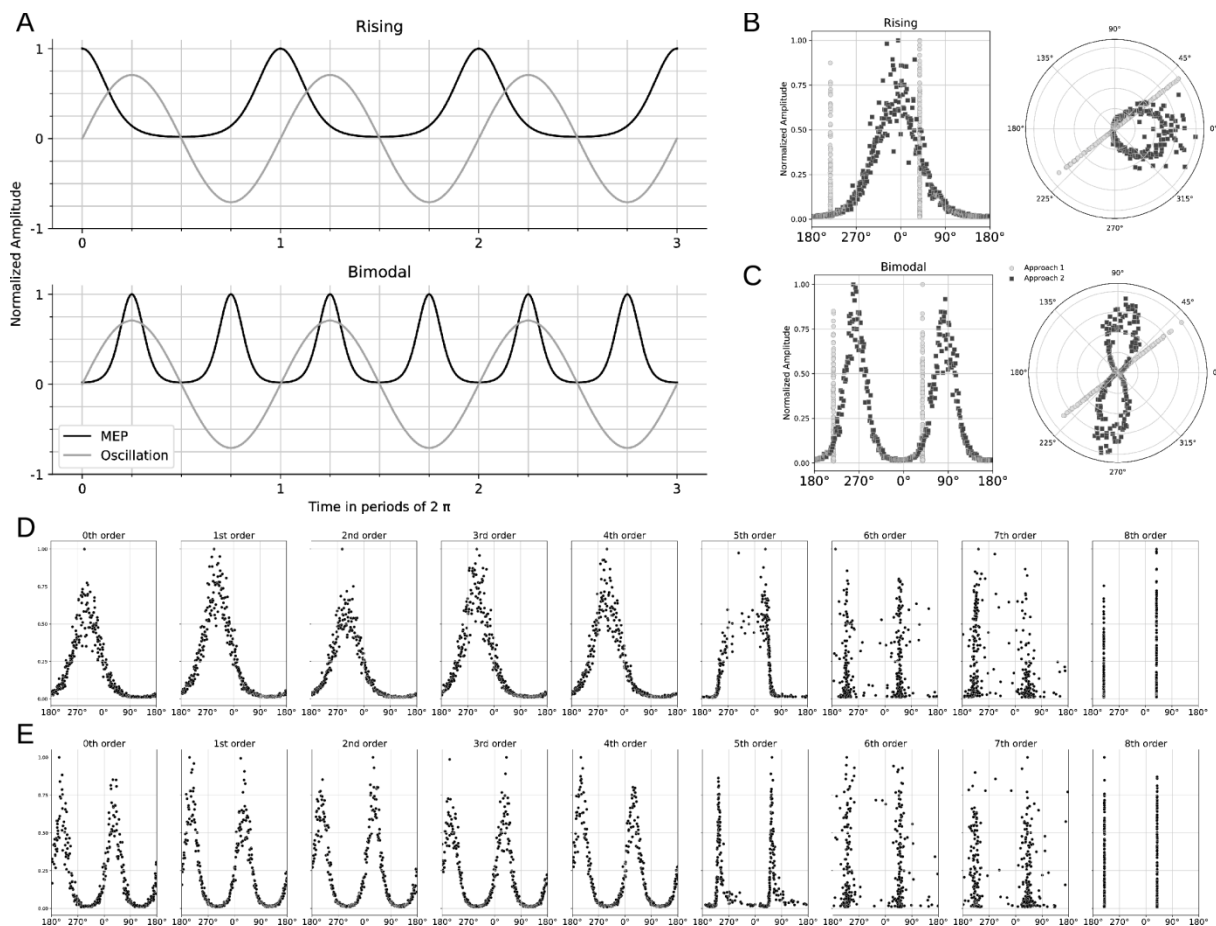
201 Findings can become biased by too high filter orders or uneven pass-bands. On a
202 more general account, these observations propose two approaches: (i) Using up-to-
203 date toolboxes and re-running scripts after software updates (Kitzes et al., 2018) and
204 (ii) Running simulation studies in parallel to the actual data processing to safeguard
205 the analysis pipeline against potential pitfalls (Haufe, 2015).

206

207 References

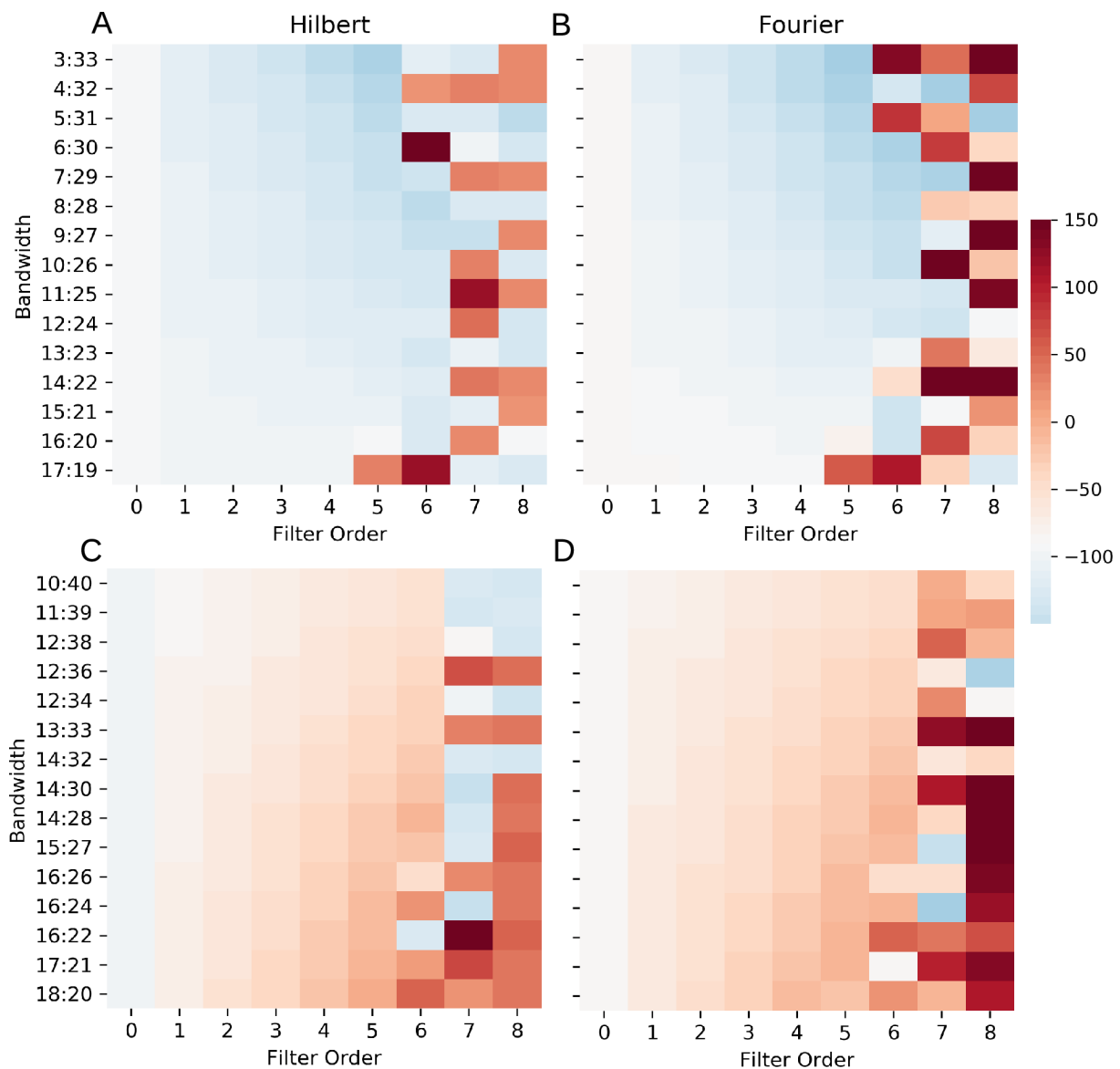
- Cole, S.R., Voytek, B., 2017. Brain Oscillations and the Importance of Waveform Shape. *Trends Cogn. Sci.* 21, 137–149. <https://doi.org/10.1016/j.tics.2016.12.008>
- Fehér, K.D., Nakataki, M., Morishima, Y., 2017. Phase-Dependent Modulation of Signal Transmission in Cortical Networks through tACS-Induced Neural Oscillations. *Front. Hum. Neurosci.* 11. <https://doi.org/10.3389/fnhum.2017.00471>
- Gharabaghi, A., Kraus, D., Leão, M.T., Spüler, M., Walter, A., Bogdan, M., Rosenstiel, W., Naros, G., Ziemann, U., 2014. Coupling brain-machine interfaces with cortical stimulation for brain-state dependent stimulation: enhancing motor cortex excitability for neurorehabilitation. *Front. Hum. Neurosci.* 8, 122. <https://doi.org/10.3389/fnhum.2014.00122>
- Guerra A, Pogosyan A, Nowak M, Tan H, Ferreri F, Di Lazzaro V, Brown P (2016) Phase dependency of the human primary motor cortex and cholinergic inhibition cancelation during beta tACS. *Cereb Cortex* 26:3977-3990.
- Haufe, S., 2015. An extendable simulation framework for benchmarking EEG-based brain connectivity estimation methodologies. *IEEE*, pp. 7562–7565. <https://doi.org/10.1109/EMBC.2015.7320142>
- Izhikevich, E.M., 2007. *Dynamical systems in neuroscience: the geometry of excitability and bursting*, Computational neuroscience. MIT Press, Cambridge, Mass.
- Keil, J., Timm, J., Sanmiguel, I., Schulz, H., Obleser, J., Schoenwiesner, M., 2013. Cortical Brain States and Corticospinal Synchronization Influence TMS-evoked motor potentials. *J. Neurophysiol.* <https://doi.org/10.1152/jn.00387.2013>
- Khademi, F., Royter, V., Gharabaghi, A., 2018. Distinct Beta-band Oscillatory Circuits Underlie Corticospinal Gain Modulation. *Cereb. Cortex* 28, 1502–1515. <https://doi.org/10.1093/cercor/bhy016>
- Kitzes, J., Turek, D., Deniz, F. (Eds.), 2018. *The practice of reproducible research: case studies and lessons from the data-intensive sciences*. University of California Press, Oakland, California.
- Kraus, D., Naros, G., Bauer, R., Khademi, F., Leão, M.T., Ziemann, U., Gharabaghi, A., 2016. Brain State-Dependent Transcranial Magnetic Closed-Loop Stimulation Controlled by Sensorimotor Desynchronization Induces Robust Increase of Corticospinal Excitability. *Brain Stimulat.* 9, 415–424. <https://doi.org/10.1016/j.brs.2016.02.007>
- Kraus D, Naros G, Guggenberger R, Leão MT, Ziemann U, Gharabaghi A. Recruitment of Additional Corticospinal Pathways in the Human Brain with State-Dependent Paired Associative Stimulation. *J Neurosci.* 2018 Feb 7;38(6):1396-1407. doi: 10.1523/JNEUROSCI.2893-17.2017.
- Nakazono H, Ogata K, Kuroda T, Tobimatsu S (2016) Phase and frequency-dependent effects of transcranial alternating current stimulation on motor cortical excitability. *PloS One* 11:e0162521.
- Oostenveld, R., Fries, P., Maris, E., Schoffelen, J.-M., 2011. FieldTrip: Open Source Software for Advanced Analysis of MEG, EEG, and Invasive Electrophysiological Data. *Comput. Intell. Neurosci.* 2011, 1–9. <https://doi.org/10.1155/2011/156869>
- Oppenheim, A.V., Willsky, A.S., Nawab, S.H., 2014. *Signals & Systems*.
- Raco, V., Bauer, R., Tharsan, S., Gharabaghi, A., 2016. Combining TMS and tACS for closed-loop phase-dependent modulation of corticospinal excitability: A feasibility study. *Front. Cell. Neurosci.* 10. <https://doi.org/10.3389/fncel.2016.00143>
- Schilberg L, Engelen T, Ten Oever S, Schuhmann T, de Gelder B, de Graaf TA, Sack AT (2018) Phase of beta-frequency tACS over primary motor cortex modulates corticospinal excitability. *Cortex* 103:142-152.
- Takahashi, K., Kato, K., Mizuguchi, N., Ushiba, J., 2018. Precise estimation of human corticospinal excitability associated with the levels of motor imagery-related EEG desynchronization extracted by a locked-in amplifier algorithm. *J. NeuroEngineeringRehabil.* 15. <https://doi.org/10.1186/s12984-018-0440-5>

- Takemi, M., Masakado, Y., Liu, M., Ushiba, J., 2013. Event-related desynchronization reflects downregulation of intracortical inhibition in human primary motor cortex 110, 1158–1166. <https://doi.org/10.1152/jn.01092.2012>
- van Elswijk, G., Maij, F., Schoffelen, J.-M., Overeem, S., Stegeman, D.F., Fries, P., 2010. Corticospinal beta-band synchronization entails rhythmic gain modulation. *J. Neurosci. Off. J. Soc. Neurosci.* 30, 4481–4488. <https://doi.org/10.1523/JNEUROSCI.2794-09.2010>
- Widmann, A., Schröger, E., Maess, B., 2015. Digital filter design for electrophysiological data--a practical approach. *J. Neurosci. Methods* 250, 34–46. <https://doi.org/10.1016/j.jneumeth.2014.08.002>
- Zaehle, T., Rach, S., Herrmann, C.S., 2010. Transcranial alternating current stimulation enhances individual alpha activity in human EEG. *PLoS One* 5, e13766. <https://doi.org/10.1371/journal.pone.0013766>
- Zrenner, C., Desideri, D., Belardinelli, P., Ziemann, U., 2017. Real-time EEG-defined excitability states determine efficacy of TMS-induced plasticity in human motor cortex. *Brain Stimulat.* <https://doi.org/10.1016/j.brs.2017.11.016>



209 **Figure 1 Recovery of uni- and bimodal models depending on the approach**
 210 **applied**

211 **A**, Upper row shows unimodal phase-dependency with maximum MEP amplitude
 212 (black line) at the rising flank of oscillatory activity (gray line). Lower row shows
 213 bimodal phase-dependency with maximum MEP amplitude (black line) at the peak
 214 and trough of oscillatory activity (gray line). **B** Unimodal phase-dependency which is
 215 not recovered by narrow-band filtering followed by Hilbert transformation (approach 1,
 216 light dots) but by broad-band filtering followed by discrete Fourier transform
 217 (approach 2, dark dots). **C** Bimodal phase-dependency which is recovered by
 218 approach 2 (dark dots) and in a distorted way by approach 1 (light dots). Left columns
 219 are scatter plots with phase on the x-axis and recovered MEP amplitude on the y-axis.
 220 Right columns show the same data as a polar plot on the unit circle. **D/E** The recovery
 221 depending on filter order for approach 1, i.e., narrow-band (17-19 Hz) filtering followed
 222 by Hilbert transformation with different filter orders (from zero to 8th) for the unimodal
 223 (E) or the bimodal (F) model. Lower filter orders can distinguish between bimodal and
 224 unimodal dependencies of MEP amplitudes. Note that, due to the estimation of the
 225 phase 5 ms prior to the TMS-pulse, a phase-shift occurs even without filtering.



226 **Figure 2 Estimated optimal phase for the unimodal dependency depends on**
 227 **filter width, center and order**

228 All heat maps show, with filter order on the x-axis and bandwidth on the y-axis, the
 229 estimated optimal phase color-coded with a divergent colormap. The colormap is
 230 anchored with white to -90, i.e., the optimal phase according to the simulation. The
 231 rows show the recovery depending on whether Hilbert (A/C) or Fourier (B/D)
 232 transformation was used for phase estimation. The columns show the recovery for
 233 evenly centered (A/B) or uneven bands (C/D).